Structural Eng./Earthquake Eng., JSCE, Vol. 14, No. 2, 185s－199s, 1997 October

ON FLUTTER STABILITY OF DECKS FOR SUPER LONG-SPAN BRIDGE

Masaru MATSUMOTO[1], Hiroshi HAMASAKI[2] and Fumitaka YOSHIZUMI[3]

[1]Member of JSCE, Dr. of Eng., Professor, Dept of Civil Eng., Kyoto University (Yoshidahonmachi, Sakyo-ku,Kyoto 606-01, Japan)
[2]Member of JECE, M. Eng., R&D Dept. Fuji Research Institute Co. (20-14, Shiba 5, Minato-ku, Tokyo 108, Japan)
[3]Member of JSCE, Graduate Student of Kyoto University (Yoshidahonmachi, Sakyo-ku, Kyoto 606-01, Japan)

Because of the increasing span lengths of suspension bridges, it has become more important to evaluate the stability of flutter phenomena.This study aims to make clearer the mechanisms of coupled flutter. In order to acomplish this, wind tunnnel tests are carried out on fundamental bluff bodies to calculate their aerodynamic derivatives. The roles of these aerodynamic derivatives are then investigated by using a step-by-step analysis in place of the conventional complex eigen value analysis.

Key Words : aerodynamic derivatives,flutter mechanism,flutter analysis,unsteady pressure

1. INTRODUCTION

Through the development of high strength steel, it has become possible to construct long span suspension bridges. In addition, with the progress of technical welding skill, energy loss due to sliding friction has decreased. As a result, both the horizontal and torsional displacements of the bridge girder have become more sensitive to external forces, and natural frequency, in addition structural damping has decreased. Therefore, aerodynamic instability tends to occur in super long-span suspension bridges more frequently than before, providing motivation to develop a superior flutter stabilization method. Thus far, many laboratories have conducted various studies of flutter mechanisms. By assuming a box shaped girder in super long-span suspension bridges, Sato et al[1] studied the effects of wind-resisting stabilization by changing the size of the grating mouth of the box girder. Kusakabe et al[2] proposed cross section and aimed to resist flutter by controlling vertical plate vibration. There are various approaches to control flutter. This study aims to discover how to control the flow pattern around the cross section and to propose a superior girder section which stabilizes flutter instability.

This paper is translated into English from the Japanese paper, which originally appeared on J. Struct. Mech. Earthpuake Eng., JSCE, No.537/I-30, pp. 191-203, 1996.4.

2. FLUTTER GENERATION MECHANISM

In general, aerodynamic force which acts on structures is classified into two types, steady aerodynamic force which doesn't change with time, and unsteady aerodynamic force which changes as time does. Furthermore, the latter is classified further into two types, compulsory aerodynamic force which is hardly affected by the vibration characteristics of structures, and motion-induced aerodynamic force which independently grows in strength by itself through vibration of structures in flow. Motion-induced vibration phenomena, such as coupled flutter instability which combines heaving vibration and torsional vibration, torsional flutter instability which is dominated by torsional vibration, galloping which is dominated by heaving vibration, and vortex-induced vibration, are ascribed to motion-induced properties of unsteady aerodynamic force. Of the motion-induced vibrations, flutter instability and galloping are very dangerous phenomena which

could destroy structures. Limiting to the girder and deck of long-span bridges, it is possible that coupled flutter and torsional flutter occur[3]. However many aspects of flutter generation mechanism are not clear yet. In order to clarify flutter generation mechanism, the authors propose (1)dependence between aerodynamic derivatives,and (2)the analysis method reflecting coupled action between torsional motion and heaving motion as follows.

(1) Unsteady aerodynamic coefficient and their dependence

When discussing flutter instability of girder cross-sections of long-span bridges, it is important to estimate the unsteady force caused by fluid (in this case wind acting on it). Unsteady lift force L and unsteady moment M which act on girder cross-sections in heaving and torsional 2DOF vibration are expressed by adopting the 8 aerodynamic derivatives as follows[4].

$$L = \frac{1}{2}\rho(2b)U^2\left\{kH_1^*\frac{\dot{\eta}}{U} + kH_2^*\frac{b\dot{\phi}}{U} + k^2H_3^*\phi + k^2H_4^*\frac{\eta}{b}\right\}, \quad (1)$$

$$M = \frac{1}{2}\rho(2b^2)U^2\left\{kA_1^*\frac{\dot{\eta}}{U} + kA_2^*\frac{b\dot{\phi}}{U} + k^2A_3^*\phi + k^2A_4^*\frac{\eta}{b}\right\}$$

in which, L: lift force per unit span (downward force is positive), M: moment per unit span (nose up is positive), η: heaving displacement (downward is positive), ϕ: torsional displacement (nose up is positive), ($\cdot$): the differential with respect to time, U: wind velocity, ρ: air density, b: half chord length, k: reduced frequency (=b ω/U), ω: circular frequency

Among the eight aerodynamic derivatives, H_1^*, H_4^*, A_2^*, A_3^* are uncoupled derivatives and H_2^*, H_3^*, A_1^*, A_4^* are coupled derivatives.

These eight aerodynamic derivatives, H_i^*, A_i^* are affected by fluctuating pressure properties. In other words, the eight coefficients are not completely independent. The authors et al have shown that following dependence exists approximately through reduced frequency k. The dependence is confirmed by experiments[5] and deduced from similarity between unsteady pressure characteristics in heaving (vertical) vibration and torsional vibration.

$$H_3^* = \frac{H_1^*}{k}, H_2^* = -\frac{H_4^*}{k}, A_3^* = \frac{A_1^*}{k}, A_2^* = -\frac{A_4^*}{k} \quad (2)$$

In addition, considering equivalent Wagner function for bluff bodies which corresponds to Wagner function for a two-dimensional thin plate, the dependence between H_1^* and H_4^*, H_2^* and H_3^*, A_1^* and A_4^*, A_2^* and A_3^* can be derived[5]. The clarification of these dependencies are shown in chapter 8.

(2) Coupled flutter generation mechanism

In 2DOF vibration systems where coupled flutter is occurring, that flutter can be reduced by restricting one of the system's motions and thereby forcing it to become 1DOF. That is, whether coupled flutter instability occurs greatly depends on the coupled action of two motions. In general, through coupled flutter analysis of heaving / torsional 2DOF vibration systems for bridge cross sections, the torsional branch (predominant mode) leads to coupled flutter, while the heaving branch (predominant mode) becomes damped down. By examining the relationship between torsional vibration and heaving vibration, and through consideration of what roles the coupling terms possess, this research aims at clarification of coupled flutter generation system. As the existence of flutter in the cross-section due to the heaving branch is reported by the authors[6], the same analysis is conducted for flutter instability which occurs by the heaving branch. **Fig 1.** shows correlation among aerodynamic derivatives on the torsional and heaving branches. Concrete clarification about this subject is discussed in chapter 8.

3. OUTLINE OF WIND TUNNEL EXPERIMENT

The cross sections used in this study are rectangular sections, an elliptical section, rectangular section with a center vertical plate, a triangle section, and a tandem isolated elliptical section as can be seen in **Fig.2**. Each model is made of wood and possess a span-length of 600 mm. In the center part of each section, pressure holes to measure pressure are arranged. Moreover, end plates to maintain two-dimensional properties are attached to each model. The wind tunnel used in the experiments is an Eiffel type wind tunnel (1.0m(h) x 0.7m(w) x 5.0m(l)) (**Fig.3**).

The model used to measure aerodynamic pressure is vibrated by a 2 DOF electric vibrator (**Fig.4**). In the 2 DOF spring supported experiments of the rectangular section (ratio of sectional length, B/D=20) which was conducted, the ratio of heaving amplitude to torsional

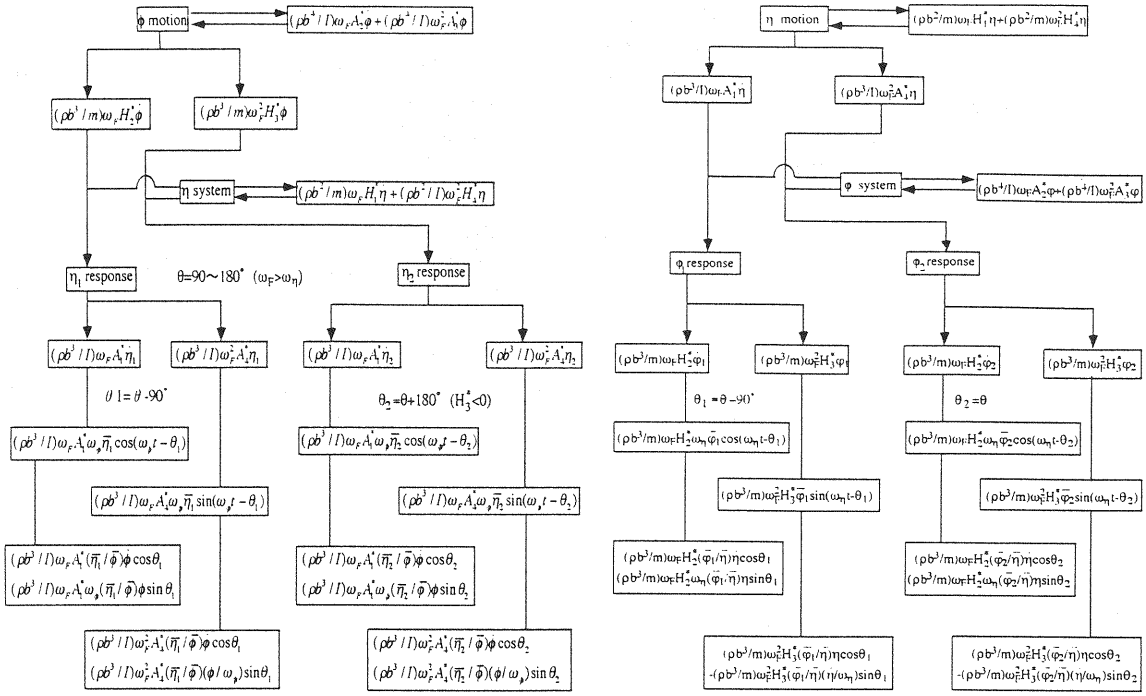

Fig.1 Correlation diagram on torsional branch (left) and heaving branch (right)

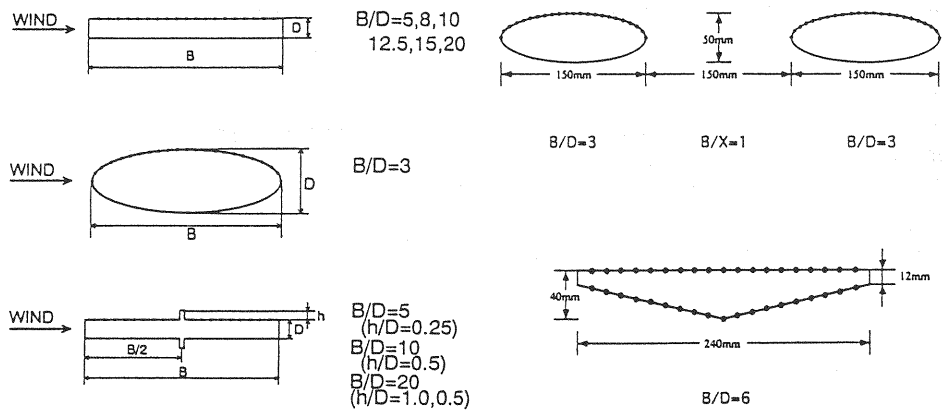

Fig.2 Cross section of model used in the experiments

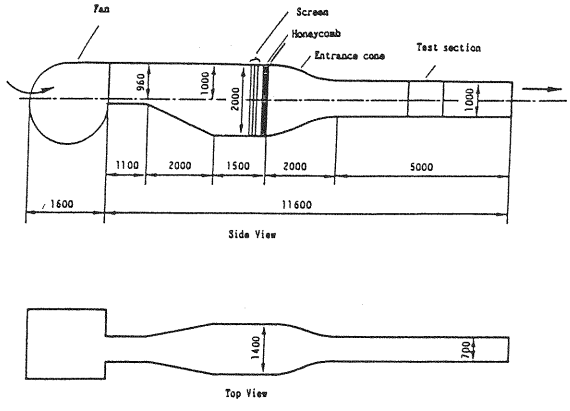

Fig.3 Wind tunnel used in the experiments

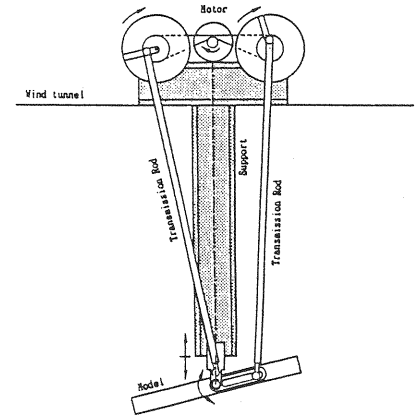

Fig.4 2DOF electric vibrator used in the experiments

amplitude, η_0/ϕ_0, was 0.1408m/rad when steady vibration of heaving / torsional coupled flutter occurred[3]. As fluctuating pressure in heaving 1DOF vibration is very small, it is necessary to set the system with the appropriate amplitude. Therefore, in this research, the double amplitude of heaving in 1DOF vibration is fixed at $2\eta_0$=10mm, and torsional amplitude of torsional 1DOF vibration is adjusted to η_0/ϕ_0=0.1408m/rad.

(1) The definition of displacement, aerodynamic force and surface pressure

In heaving (vertical) motion, downward is defined as the positive direction. Therefore, when relative pitching angle is at its maximum upward angle against the wind, downward heaving velocity is also at its maximum. At this time, the phase goes forward 90 degree from the time when heaving displacement reaches its maximum. In torsional motion, an upward, against the wind motion is defined as the positive direction. When torsional velocity in torsional 1DOF vibration is small, it can be approximated that the relative pitching angle of wind attack is torsional displacement itself. As for aerodynamic forces, downward lift force is defined as positive, as is upward moment against wind.

Unsteady pressure data obtained from the unsteady pressure measure experiment is dealt with as follows. Time integrated pressure on the pressure holes on the model surface is dealt with as the integrated pressure coefficient $\overline{C}_P$. $\overline{C}_P$ is a non-dimensional coefficient reduced by the dynamic pressure of the approaching flow. Fluctuating pressure is read as fluctuating pressure of a model-frequency component through a band-pass filter after passing through a DC amplifier. The double amplitude of fluctuating pressure is dealt with as fluctuating pressure component, $\widetilde{C}_P$, reduced by dynamic pressure. As for phase lag (ψ_B for heaving 1DOF motion and ψ_T for Torsional 1DOF motion) between displacement and fluctuating pressure, in the case of the heaving 1DOF vibration experiment, phase lag from the downward maximum of heaving velocity to the minimum of pressure (the maximum of negative pressure) on the model-upper-surface is defined to be positive. As for the case of torsional 1DOF vibration, phase lag from the maximum upward torsional displacement against the approaching flow to the maximum negative pressure on model-upper-surface is defined to be positive.

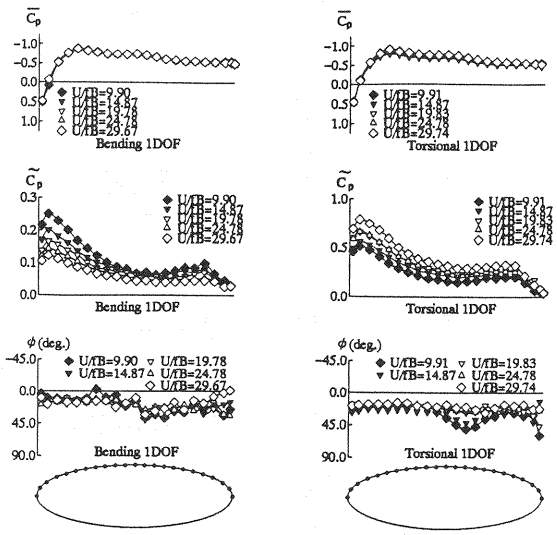

Fig.5 Fluctuating pressure properties of the elliptical section

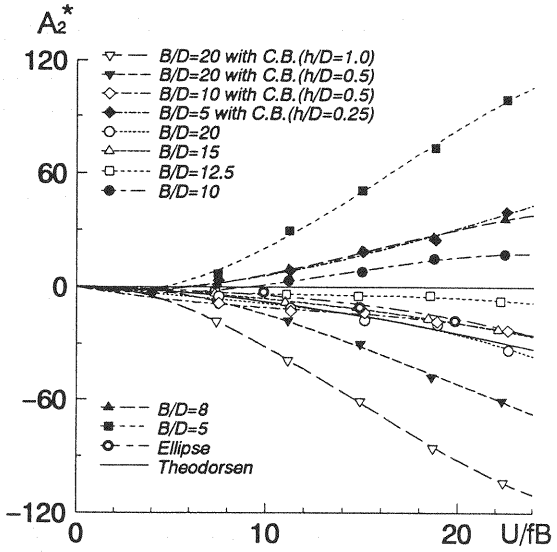

Fig.6 Aerodynamic derivatives A_2^*

4. THE AERODYNAMIC PROPERTIES OF ELLIPTICAL SECTION

Fig.5 shows fluctuating pressure properties of the elliptical section. It is assumed that the wind blows from the right. Fluctuating pressure component $\widetilde{C}_P$ has two peaks, one in the first half, and one in the second. Therefore, it is believed that two separation points exist in the leading side and the trailing side. Phase lag is approximately constant from the upper stream edge to the lower stream. Aerodynamic derivatives are calculated by use of

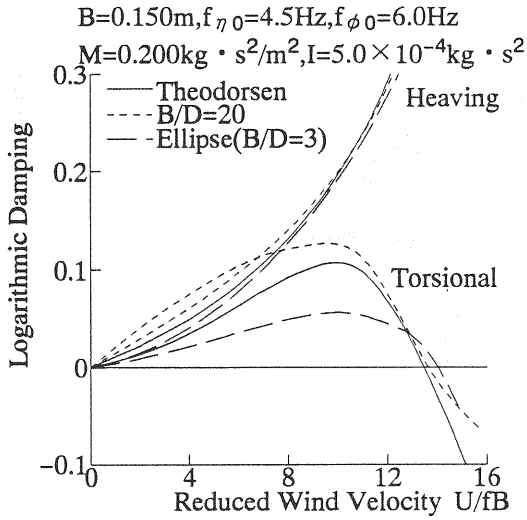

Fig.7 Complex eigen-value analysis results for the elliptical section

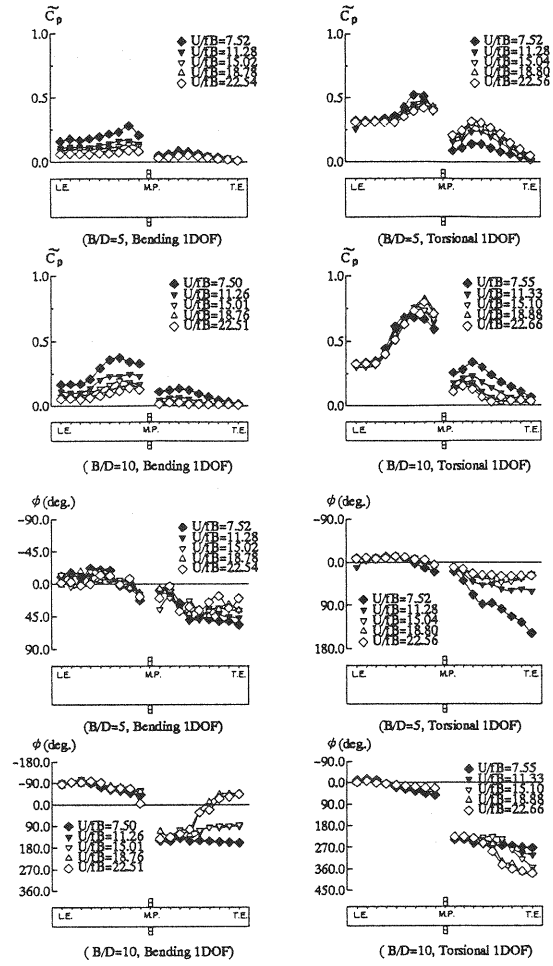

Fig.8 Fluctuating pressure properties of the rectangular section with vertical plate

these fluctuating pressure properties. **Fig.6** shows A_2^* which is considered to contribute to flutter stability among aerodynamic derivatives. If the value of A_2^* is positive, 1DOF torsional flutter occurs, and if the value A_2^* is negative, it is possible that coupled flutter occurs. In general, the former is the case of a bluff rectangular section, As the section is slender, the type of vibration becomes the latter case. Flutter onset velocity of the latter case is larger than of the former. In the elliptical section, A_2^* maintains a negative value. This is caused by the phase delay of pressure near the separation bubble of the leading edge side in the case of torsional 1DOF vibration. As A_2^* is negative, the flutter type produced is coupled flutter. The complex eigen value analysis method is conducted by use of 8 derivatives calculated from experimentation. In the complex eigen value analysis, structural damping is assumed 0, and fundamental structural value (width of section B, bending natural frequency $f_{\eta 0}$, torsional natural frequency $f_{\phi 0}$, mass per unit length M, moment inertia I) are given in **Fig.7**. For reference, the analysis of the rectangular section with B/D=20 obtained by forced vibration experiments as well as the result for the elliptical section and a two dimensional plate from Theodorsen function are also shown. The flutter onset velocity of the elliptical section is approximately the same as that of the rectangular section with B/D=20. Considering that the slenderness ratio of this elliptical section is 3 B/D=3, it is found that the elliptical section is effective to stabilize flutter.

5. THE AERODYNAMIC PROPERTIES OF RECTANGULAR SECTION WITH A VERTICAL PLATE

Fig.8 shows fluctuating pressure properties. Fluctuating pressure coefficient, $\widetilde{C}_P$ of a rectangular section with a vertical plate (center barrier, C.B.) has two peaks, one in the first half and one in the second of the surface of the section. Similar results can be seen in the elliptical section. The phase lag of the rectangular section with B/D=10 has a phase delay of 180 deg. after flow passes the C.B.. However the phase lag of a

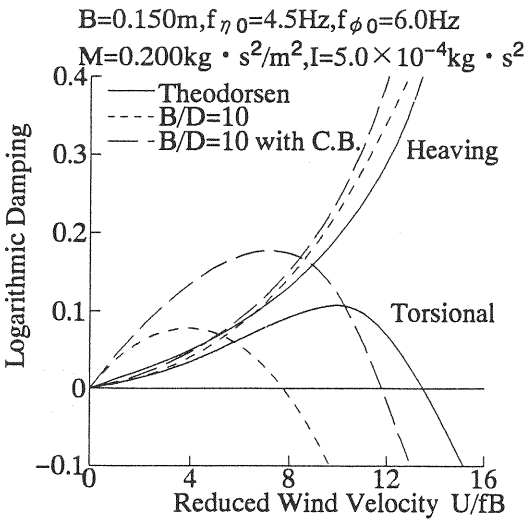

Fig.9 Complex eigen-value analysis results for the rectangular section with vertical plate

rectangular section with B/D=5 has no phase delay at the C.B.. In the case of B/D=5, it is believed that separation of flow caused by the leading edge has control over the flow pattern of the section. **Fig.6** shows A_2^*. **Fig.9** shows the result of the complex eigen value analysis taking no account of structural damping. Therefore, it is understood that flutter onset velocity becomes higher and a rectangular section with a C.B. is effective to stabilize flutter.

6. THE AERODYNAMIC PROPERTIES OF TRIANGULAR SECTION

Fig.10 shows fluctuating pressure properties of a triangular section. The properties of fluctuating pressure coefficients $\widetilde{C}_P$ on the surface of this section are approximately the same as those of the rectangular section with B/D=15 and 20. However, the fluctuating pressure coefficients of the lower are approximately 0. After the second pressure hole, the fluctuation of pressure is very small. **Fig.11** shows A_2^*. In order to compare the results of this section with that of another section, the results of the rectangular section with B/D=20 is also shown in **Fig.11**. **Fig .12** shows the results of the eigen value analysis calculated without regarding structural damping. Taking into account of the fact that the slenderness ratio, B/D of this triangular section is 6, this section has the advantage of stabilization.

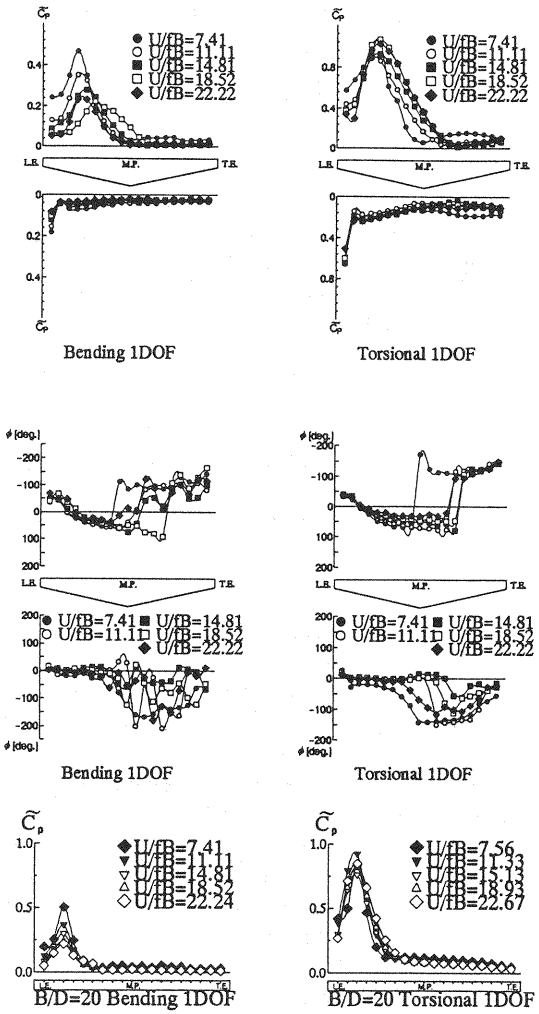

Fig.10 Fluctuating pressure properties of the triangular section

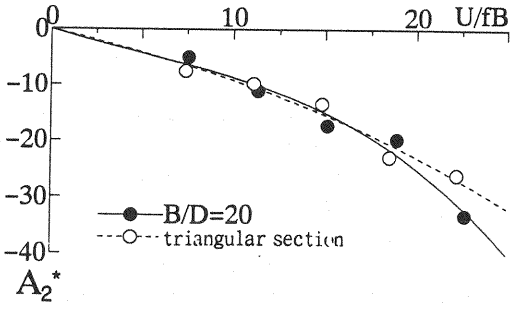

Fig.11 Aerodynamic derivatives A_2^* of the triangular section

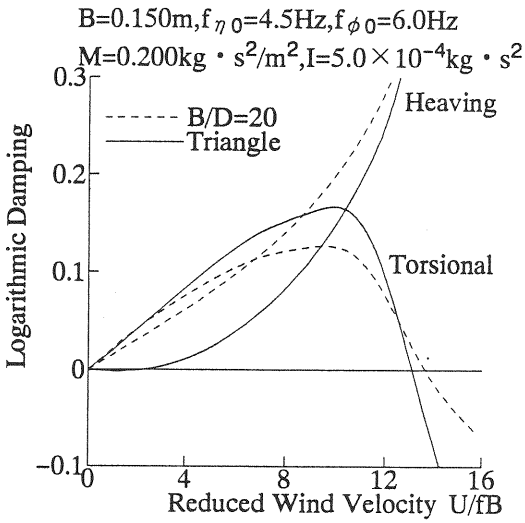

Fig.12 Complex eigen-value analysis results for the triangular section

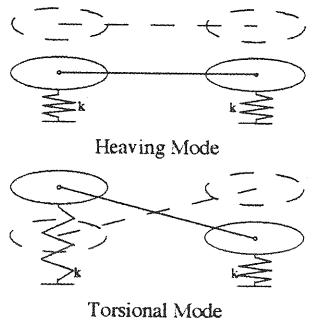

Fig.13 Heaving vibration and torsional vibration of tandem elliptical section

7. THE AERODYNAMIC PROPERTIES OF A TANDEM ELLIPTICAL SECTION

The aerodynamic properties of a simple elliptical section depends on the Reynolds number. Therefore, wind-velocity is fixed at about 8m/s, and forced vibration experiments are conducted at 5 reduced velocities U/fB (U: wind velocity, f: frequency, B: full chord length) in accordance with vibration frequencies f=1.8Hz, 2.16Hz, 2.7Hz, 3.6Hz, 5.4Hz. Following the concept of Twin-bridge proposed by Richardson, heaving (vertical) vibration and torsional vibration are fixed as **Fig.13** shows. In this vibration mode, both heaving and torsional vibration are expressed by each heaving vibration of the ellipse, and it is possible to let the ratio of natural frequency of heaving and torsional approach 1. In the case of heaving vibration, relative pitching angle of attack reaches a maximum when downward velocity is maximized. In the case of torsional vibration, it is defined that relative pitching angle becomes a maximum when the leading side body reaches the top position (that is, the trailing side body reaches the bottom position). The phase lag between the displacement of the section and fluctuating pressure is defined as the lag from the maximum relative pitching angle to the minimum pressure of the upper surface of the model. **Fig.14** shows the distribution of fluctuating pressure coefficients $\widetilde{C}_P$ in the case of heaving 1DOF vibration and 1DOF torsional vibration. In both cases, the fluctuating pressure coefficients $\widetilde{C}_P$ of both the leading side and the trailing side have 2 peaks regardless of wind velocity. The result of the leading side section is approximately the same as that of a simple elliptical section. The trailing side section has a larger peak near its leading edge than the leading side section, but in both sections, the peak near the trailing edge is approximately the same. **Fig.15** shows the phase lag. In the case of heaving vibration, the phase lag of the leading side body is almost constant from the leading edge to the trailing edge like the simple elliptical section, while the phase lag of the trailing side body proceeds from the leading edge to the trailing edge. In the case of the torsional vibration, the phase lag is constant like the simple elliptical body. The phase lag of the trailing side body proceeds from the leading edge to the center of the body and suddenly delays at that point. 8 aerodynamic derivatives are calculated considering aerodynamic forces which act on the leading and trailing side bodies as shown in **Fig.16**. Taking into account of the influence of the ratio of the heaving-torsional natural frequency ($f_{\phi 0}/f_{\eta 0}$), the complex eigen value analysis is conducted according to the change of $f_{\phi 0}/f_{\eta 0}$(**Fig.17**). (Following other analyses, structural damping is assumed 0.) In the case of the vibration mode of a tandem elliptical section assumed by this study, flutter instability does not occur in any ratio of frequencies. As reference data, the complex eigen value analysis for the rectangular section with B/D=20 is also conducted. **Fig.18** shows this result. In the case of a rectangular section with B/D=20, flutter instability does not occur in the case where $f_{\phi 0}/f_{\eta 0}=1$, but does occur in all other cases. It is believed that the tandem elliptical section is effective to stabilize flutter in the assumed vibratiion mode. It is conjectured that the lift force of bothsections caused by heaving velocity

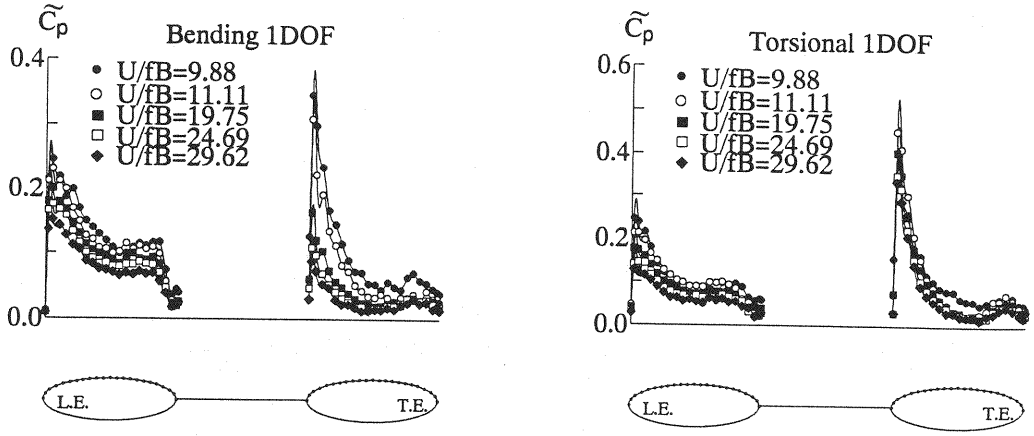

Fig.14 Fluctuating pressure properties (fluctuating pressure coefficients) of tandem elliptical section

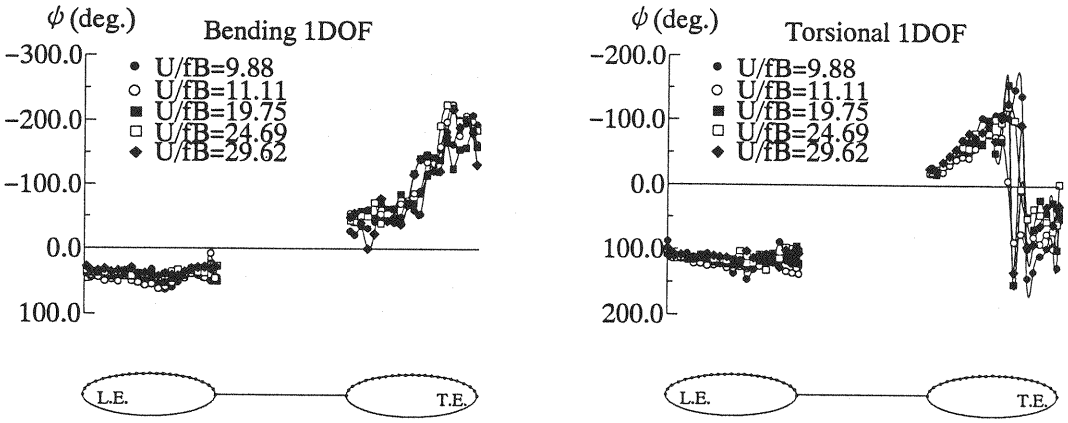

Fig.15 Fluctuating pressure properties (phase lag) of tandem elliptical section

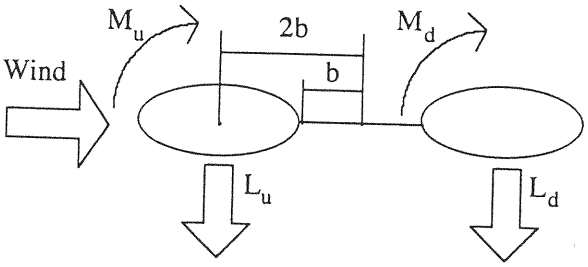

Fig.16 Aerodynamic forces which act on tandem elliptical section

in torsional motion contributes to the aerodynamic damping in torsional motion and the lift force of both sections caused by torsional displacement cancel out each other. However it is difficult to truly recreate the assumed vibrational mode in an actual bridge, and necessary to further investigate this point for practical use.

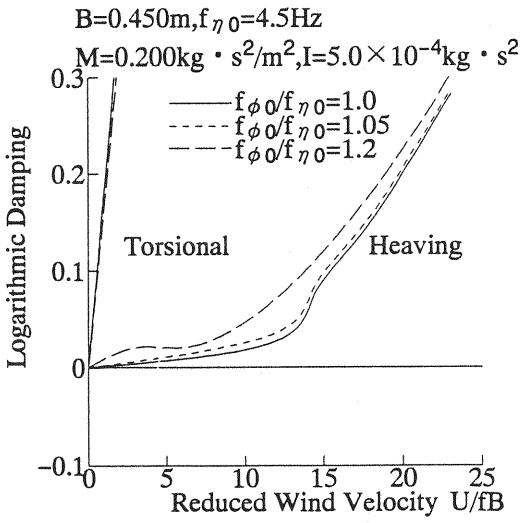

Fig.17 Complex eigen-value analysis result for tandem elliptical section

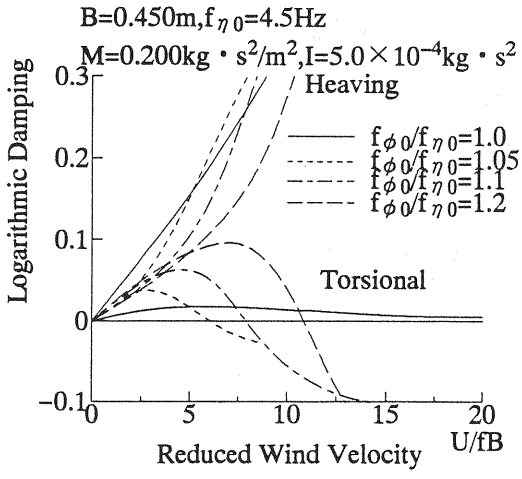

Fig.18 Effect of torsional/heaving natural frequency ratio of rectangular section with B/D=20

8. THE MECHANISM OF COUPLED-FLUTTER AND ITS STABILIZATION

In order to clarity the mechanisms of coupled flutter, so called "step-by-step" analysis and the dependence of aerodynamic derivatives were examined as follows.

(1) Step-by-step analysis

The flutter characteristics, damping and frequency are in general obtained by the complex eigen value analysis. However, this method can not define the individual role of the 8 aerodynamic derivatives. Thus, the"step-by-step"method has been developed by the author[7]. This method aims to clarify the roles of derivatives and their relationship between torsional motion and heaving motion by considering what roles coupling terms A_1^*, A_4^*, H_2^*, H_3^* possess. This analysis is respectively carried out in both a torsional branch and heaving branch. The flow charts of the step by step method for heaving and torsional branches are shown in **Fig.1**.

In the case of the torsional branch (predominant mode) the analysis is conducted as follows. Taking no account of structural damping, the equation of motion for 1DOF torsional motion is expressed as follows by rearranging eq.(1):

$$\ddot{\phi}+\omega_{\phi 0}^2\phi=(\rho b^4/I)\omega_F A_2^*\dot{\phi}+(\rho b^4/I)\omega_F^2 A_3^*\phi \quad (3)$$

in which

$\omega_{\phi 0}$: torsional natural angular frequency, ω_F: flutter angular frequency, I: moment of inertia per unit span.

Moving the right terms to the left, eq.(3) yields the following form:

$$\ddot{\phi}+2\zeta_\phi\omega_\phi\dot{\phi}+\omega_\phi^2\phi=0 \quad (4)$$

Finally, by repeated calculation, ω_ϕ becomes equal to ω_F. The equation of motion for heaving vibration caused by the torsional vibration expressed as eq.(4) can be written as follows:

$$\ddot{\eta}+\omega_{\eta 0}^2\eta=(\rho b^2/m)\omega_F H_1^*\dot{\eta}+(\rho b^3/m)\omega_F H_2^*\dot{\phi}+(\rho b^3/m)\omega_F^2 H_3^*\phi+(\rho b^2/m)\omega_F^2 H_4^*\eta \quad (5)$$

in which

$\omega_{\eta 0}$: heaving natural angular frequency, m: mass per unit span.

Moving the first and fourth terms of the right to the left, eq.(5) yields the following form:

$$\ddot{\eta}+2\zeta_\eta\omega_\eta\dot{\eta}+\omega_\eta^2\eta=(\rho b^3/m)\omega_F H_2^*\dot{\phi}+(\rho b^3/m)\omega_F^2 H_3^*\phi \quad (6)$$

In the case where the prism oscillates in 1DOF torsional motion, the following forms can be ascribed to the displacement of torsional motion:

$$\phi=\bar{\phi}\sin\omega_F t \quad (7)$$

In eq.(6) the response η_1 caused by ϕ and the response η_2 caused by ϕ is obtained as follows:

$$\eta_1=\frac{(\rho b^3/m)\omega_F^2|H_2^*|\bar{\phi}\cos(\omega_F t-\theta)}{\sqrt{(\omega_\eta^2-\omega_F^2)^2+4\zeta_\eta^2\omega_\eta^2\omega_F^2}}=\frac{(\rho b^3/m)\omega_F^2|H_2^*|\bar{\phi}\sin(\omega_F t-\theta_1)}{\sqrt{(\omega_\eta^2-\omega_F^2)^2+4\zeta_\eta^2\omega_\eta^2\omega_F^2}} \quad (8)$$

$$\eta_2=\frac{(\rho b^3/m)\omega_F^2|H_3^*|\bar{\phi}\sin(\omega_F t-\theta)}{\sqrt{(\omega_\eta^2-\omega_F^2)^2+4\zeta_\eta^2\omega_\eta^2\omega_F^2}}=\frac{(\rho b^3/m)\omega_F^2|H_3^*|\bar{\phi}\sin(\omega_F t-\theta_2)}{\sqrt{(\omega_\eta^2-\omega_F^2)^2+4\zeta_\eta^2\omega_\eta^2\omega_F^2}}$$

where

$$\theta=\tan^{-1}\left(\frac{2\zeta_\eta\omega_\eta\omega_F}{\omega_\eta^2-\omega_F^2}\right),\quad \theta_1=\theta-\frac{\pi}{2}\ (H_2^*>0),\quad \theta_1=\theta+\frac{\pi}{2}\ (H_2^*<0)$$

$\theta_2=\theta+\pi$ (because in general H_3^* is negative)

Taking account of the coupled force caused by the heaving motion expressed as eq.(8), the equation of motion for the torsional vibration is found to be

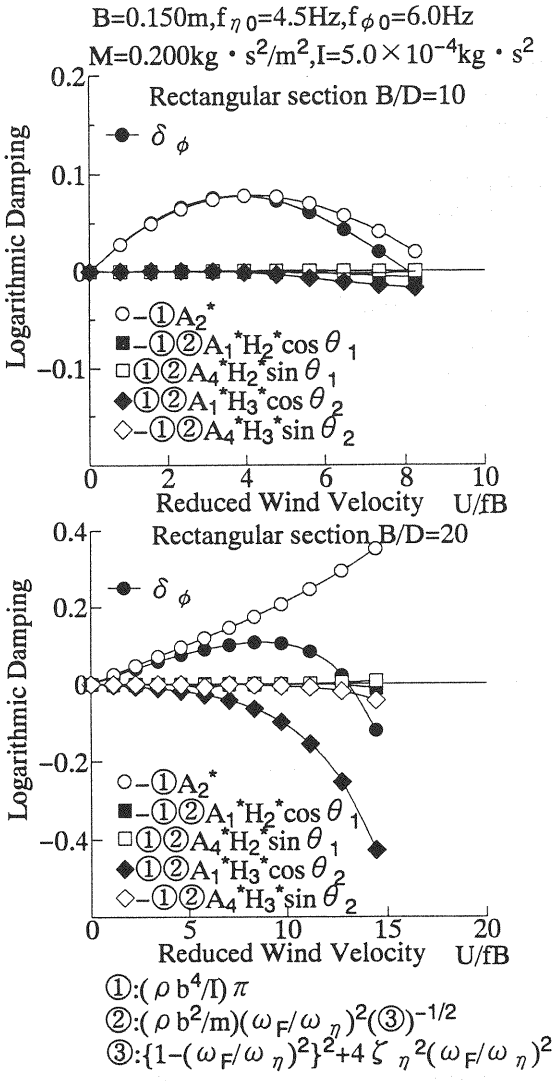

Fig.19 Step-by-step analysis results (torsional branch)

$$\ddot{\phi}+\omega_{\phi 0}^2\phi=(\rho b^4/I)\omega_F A_2^*\dot{\phi}+(\rho b^4/I)\omega_F^2 A_3^*\phi$$
$$+(\rho b^3/I)\omega_F A_1^*(\dot{\eta}_1+\dot{\eta}_2)+(\rho b^3/I)\omega_F^2 A_4^*(\eta_1+\eta_2) \quad (9)$$

Substituting eq.(8) into eq.(9) and summing up multipliers for ϕ yield the damping coefficient of torsional vibration where coupled force is taken into account. By multiplying the damping coefficient by (π/ω_F), the logarithmic damping δ_ϕ for torsional motion where coupled force is taken into account can be written as follows:

$$-\delta_\phi=①A_2^*$$
$$+①②A_1^*H_2^*\cos\theta_1+①②A_1^*|H_3^*|\cos\theta_2 \quad (10)$$
$$-①②A_4^*H_2^*\sin\theta_1-①②A_4^*|H_3^*|\sin\theta_2$$

in which

①: $(\rho b^4/I)\pi$, ②: $(\rho b^2/m)(\omega_F/\omega_\eta)^2(③)^{-1/2}$,

③: $\left\{1-(\omega_F/\omega_\eta)^2\right\}^2+4\zeta_\eta^2(\omega_F/\omega_\eta)^2$

In the case of the heaving predominant mode, an analysis similar to the case of the torsional branch is carried out as follows. Taking no account of structural damping, eq(1) is rearranged to express the equation of motion for 1DOF heaving motion as follows:

$$\ddot{\eta}+\omega_{\eta 0}^2\eta=(\rho b^2/m)\omega_F H_1^*\dot{\eta}+(\rho b^2/m)\omega_F^2 H_4^*\eta \quad (11)$$

Moving the right terms to the left, eq.(11) yields the following form:

$$\ddot{\eta}+2\zeta_\eta\omega_\eta\dot{\eta}+\omega_\eta^2\eta=0 \quad (12)$$

With repeated calculation, ω_η finally becomes equal to ω_F. The equation of motion for torsional vibration caused by the heaving vibration expressed as eq.(12) can be written as follows:

$$\ddot{\phi}+\omega_{\phi 0}^2\phi=(\rho b^3/I)\omega_F A_1^*\dot{\eta}+(\rho b^4/I)\omega_F A_2^*\dot{\phi}$$
$$+(\rho b^4/I)\omega_F^2 A_3^*\phi+(\rho b^3/I)\omega_F^2 A_4^*\eta \quad (13)$$

Moving the first and fourth term of the right to the left, we get

$$\ddot{\phi}+2\zeta_\phi\omega_\phi\dot{\phi}+\omega_\phi^2\phi=(\rho b^3/I)\omega_F A_1^*\dot{\eta}+(\rho b^3/I)\omega_F^2 A_4^*\eta \quad (14)$$

Heaving displacement can be written as follows:

$$\eta=\bar{\eta}\sin\omega_F t \quad (15)$$

In eq.(14) the response ϕ_1 caused by $\dot{\eta}$ and the response ϕ_2 caused by η is obtained as follows:

$$\phi_1=\frac{(\rho b^3/I)\omega_F^2 A_1^*\bar{\eta}\cos(\omega_F t-\theta)}{\sqrt{(\omega_\phi^2-\omega_F^2)^2+4\zeta_\phi^2\omega_\phi^2\omega_F^2}}=\frac{(\rho b^3/I)\omega_F^2|A_1^*|\bar{\eta}\sin(\omega_F t-\theta_1)}{\sqrt{(\omega_\phi^2-\omega_F^2)^2+4\zeta_\phi^2\omega_\phi^2\omega_F^2}} \quad (16)$$

$$\phi_2=\frac{(\rho b^3/I)\omega_F^2 A_4^*\bar{\eta}\sin(\omega_F t-\theta)}{\sqrt{(\omega_\phi^2-\omega_F^2)^2+4\zeta_\phi^2\omega_\phi^2\omega_F^2}}=\frac{(\rho b^3/I)\omega_F^2|A_4^*|\bar{\eta}\sin(\omega_F t-\theta_2)}{\sqrt{(\omega_\phi^2-\omega_F^2)^2+4\zeta_\phi^2\omega_\phi^2\omega_F^2}}$$

where

$$\theta=\tan^{-1}\left(\frac{2\zeta_\phi\omega_\phi\omega_F}{\omega_\phi^2-\omega_F^2}\right),\ \theta_1=\theta-\frac{\pi}{2}\ (A_1^*>0),\ \theta_1=\theta+\frac{\pi}{2}\ (A_1^*<0)$$

$\theta_2=\theta$ $(A_4^*>0)$, $\theta_2=\theta+\pi$ $(A_4^*<0)$

Taking account of the coupled force caused by

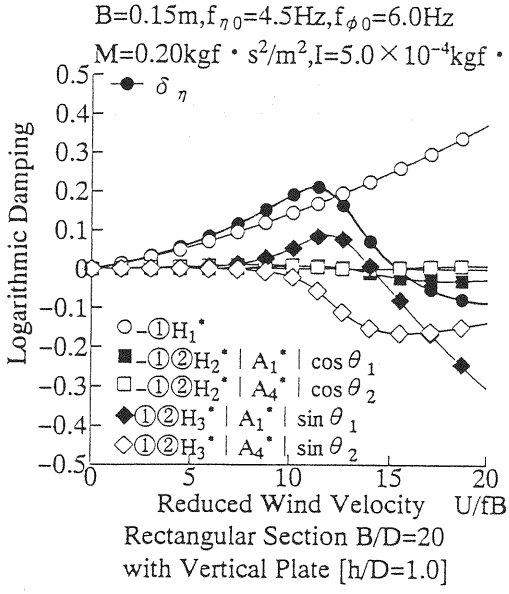

Fig.20 Step-by-step analysis results (heaving branch)

the torsional motion expressed as eq.(16), the equation of motion for the heaving vibration is found to be

$$\ddot{\eta}+\omega_{\eta 0}^2\eta=(\rho b^2/m)\omega_F H_1^*\dot{\eta}+(\rho b^2/m)\omega_F^2 H_4^*\eta$$
$$+(\rho b^3/m)\omega_F H_2^*(\dot{\phi}_1+\dot{\phi}_2)+(\rho b^3/m)\omega_F^2 H_3^*(\phi_1+\phi_2) \quad (17)$$

Substituting eq.(16) into eq.(17) and summing up multipliers for $\dot{\eta}$ yield the damping coefficient of heaving vibration where coupled force is taken into account. By multiplying the damping coefficient by (π/ω_F), the logarithmic damping δ_η for heaving motion where coupled force is taken into account can be written as follows:

$$-\delta_\eta = ①H_1^*$$
$$+①②|A_1^*|H_2^*\cos\theta_1+①②|A_4^*|H_2^*\cos\theta_2$$
$$-①②|A_1^*|H_3^*\sin\theta_1-①②|A_4^*|H_3^*\sin\theta_2 \quad (18)$$

where

$$①: (\rho b^2/m)\pi,\ ②: (\rho b^4/I)(\omega_F/\omega_\phi)^2(③)^{-1/2},$$
$$③: \left\{1-(\omega_F/\omega_\phi)^2\right\}^2+4\zeta_\phi^2(\omega_F/\omega_\phi)^2$$

The flow charts for these analyses are shown in **Fig.1**. The result of the step by step analysis which is carried out for the case that flutter develops from the torsional branch is shown in **Fig.19**. It is clear that in the case where B/D is small, A_2^* has control over developing flutter and this type of flutter is classified as torsional flutter. On the other hand, where B/D is large, the term ① ②$A_1^*H_3^*\cos\theta_2$ has control and this type of response is classified as coupled flutter. Therefore, it is clear that the coupling terms A_1^* and H_3^* play important roles in coupled flutter. The authors gave one example of the case where flutter develops from the heaving branch (rectangular section with B/D=20 with a center vertical plate). The results of the step-by-step analysis carried out for this case is shown in **Fig.20**. Here, it is clear that the term ①②$A_1^*H_3^*\sin\theta_1$ takes control. In this case, the coupling terms A_1^* and H_3^* play important parts as well. Therefore, it is concluded that flutter develops from both the torsional and heaving branchs with the coupling terms A_1^* and H_3^* playing particularly important roles.

(2) Dependence of aerodynamic derivatives

In this paragraph, the appropriateness of the dependence between aerodynamic derivatives which was suggested in chapter 2 is examined.

a) Dependence obtained by mediation of reduced frequency k.

The experimentally confirmed similarity of unsteady pressure characteristics between heaving and torsional motions leads to the dependence of aerodynamic derivatives as follows:

$$H_3^*=H_1^*/k,\ H_2^*=-H_4^*/k,\ A_3^*=A_1^*/k,\ A_2^*=-A_4^*/k \quad (2)$$

k: reduced frequency ($k=b\omega/U$)

The results of the examination of this dependence between derivatives obtained by forced vibration experiments is shown in **Fig.21**. It becomes clear that the dependence expressed as eq.(2) is rather appropriate. In **Fig.21**, it is observed that there are gaps between H_2^* and $-H_4^*/k$, A_2^* and $-A_4^*/k$. It is thought that this is because of errors in the measurement of H_4^* and A_4^*. The dependence expressed as eq.(2) holds true for all rectangular sections shown in **Fig.2**, though only two cases are shown in **Fig.21**. Therefore, it is clear that in cases of rectangular sections with side ratios larger than B/D=5, there is not much difference between unsteady pressure characteristics per unit angle of attack of heaving motion and torsional motion. In addition, torsional velocity has no effect on unsteady aerodynamic characteristics. The result of this eigen value analysis considering eq.(2)is shown in **Fig.22**. In **Fig.22**, the solid line shows the result for the case where the experimental data is

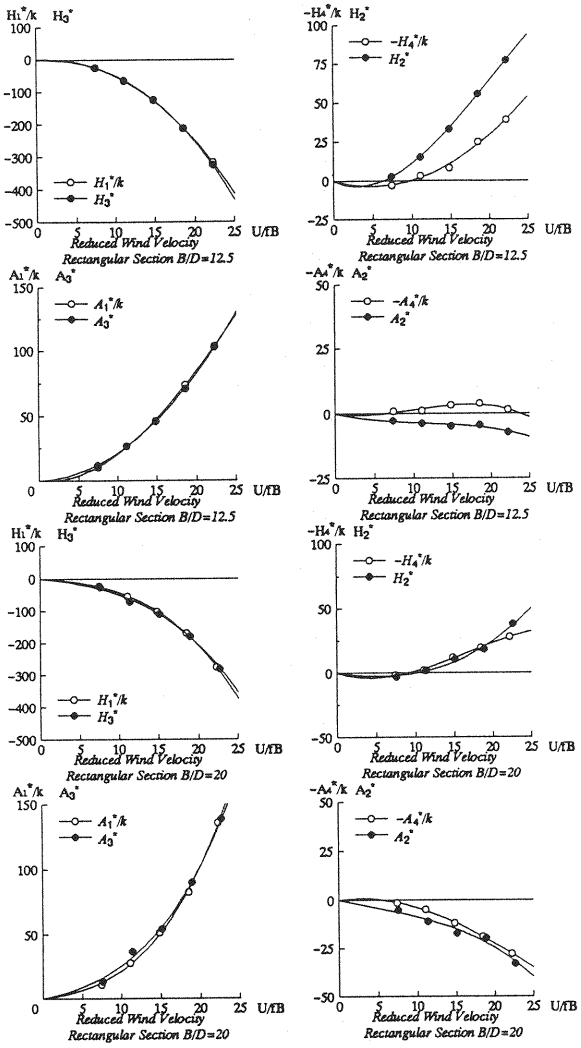

Fig.21 Dependence between aerodynamic derivatives by mediation of reduced frequency k

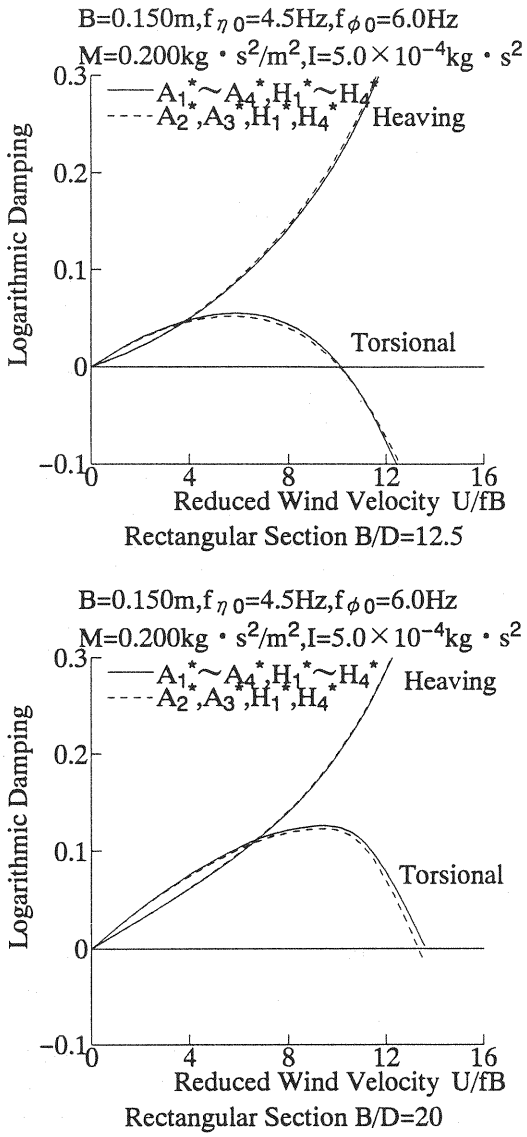

Fig.22 Complex eigen-value analysis result in the case of using dependence between aerodynamic derivatives by mediation of reduced frequency k

applied to all 8 derivatives H_1^*~H_4^* and A_1^*~A_4^*. The dotted line shows the result of the case where experimental data is applied to the 4 non-coupled derivatives H_1^*, H_4^*, A_2^*, A_3^* and the other 4 coupling derivatives are calculated from the 4 non-coupling derivatives by use of eq.(2). In the latter case, the number of derivatives which should be obtained by experimentation decreases from 8 to 4. **Fig.22** also shows that the dotted line coincides with the solid line. Therefore, it is concluded that the dependence expressed as eq.(2) can be applied to the eigen value analysis and if 4 non-coupled derivatives are measured correctly, the eigen value method can analyze flutter property by use of eq.(2).

b) Dependence obtained by mediation of equivalent Wagner function

The dependence between A_2^* and A_3^* and between H_1^* and H_4^* is obtained by considering the equivalent Wagner function. Employing the dependence based on the equivalent Wagner function and the reduced frequency as shown in the last paragraph (a), the number of the final independent aerodynamic derivatives is 2.

That is, 3 derivatives among H_i^* (i=1~4) can be calculated from the remainder and 3 among A_i^*

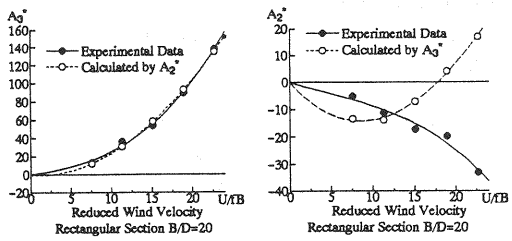

Fig.23 Dependence between aerodynamic derivatives by mediation of equivalent Wagner function

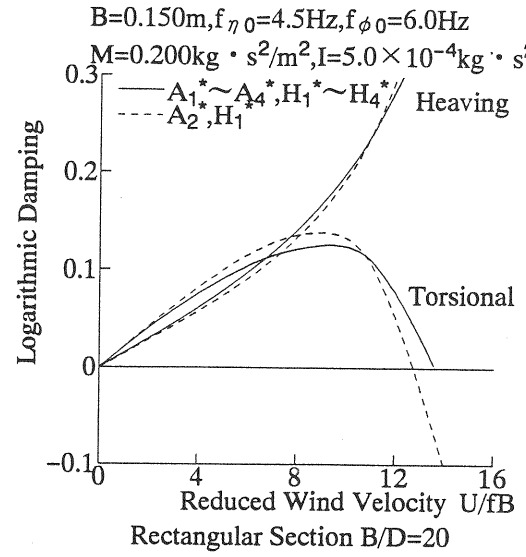

(i=1~4) its remainder. The result of this examination of the dependence based on the equivalent Wagner function is shown in **Fig.23**. In this figure, there is a little gap between the experimental value of A_3^* and the value of A_3^* calculated from the experimental value of A_2^* by use of the equivalent Wagner function. On the other hand, there is a gap between the experimental value of A_2^* and the value of A_2^* calculated from the experimental value of A_3^*. The reason the dependence based on the equivalent Wagner function holds true in the former case and not in the latter case is considered the problem of accuracy in the choice of the equivalent Wagner function. The results of the complex eigen value analysis considering eq.(2) and the dependence based on the equivalent Wagner function is shown in **Fig.24**. In **Fig.24**, the solid line shows the result of the case where the experimental data is applied to all 8 derivatives. The dotted line shows the results for the case where experimental data is applied to H_1^* and $A_2^*(A_3^*)$, and the other 6 derivatives are calculated from the experimental value of H_1^* and $A_2^*(A_3^*)$ by use of the two dependence relationships. However, in the case where the experimental data is applied to H_1^* and A_3^*, the solid lines and the dotted lines do not coincide with each other. In the case where the experimental data is applied to H_1^* and A_2^*, both of the lines coincide with each other. Therefore, it is concluded that the dependence based on the equivalent Wagner function can be applied to the eigen value analysis if the equivalent Wagner function is determined accurately.

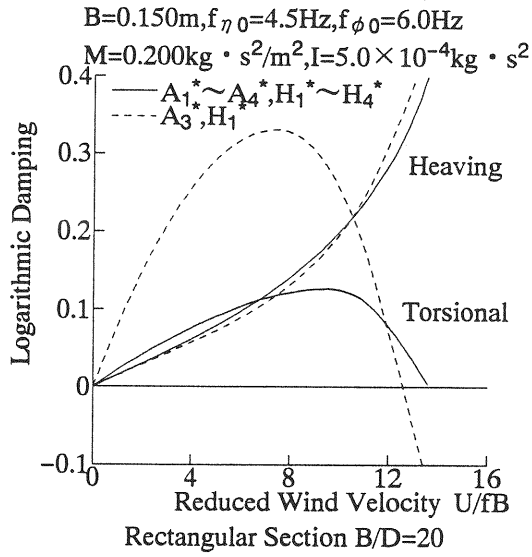

Fig.24 Complex eigen-value analysis result in the case of using dependence between aerodynamic derivatives by mediation of equivalent Wagner function

(3) The effects of the ratio of heaving and torsional natural frequency on the branch from which flutter develops

It was reported that flutter develops from the heaving branch in the case of a rectangular section, B/D=20 with a vertical plate(h/D=1.0). In this paragraph, whether or not this section changes the branch from which flutter develops in the case where the ratio between heaving and torsional natural frequency changes will be

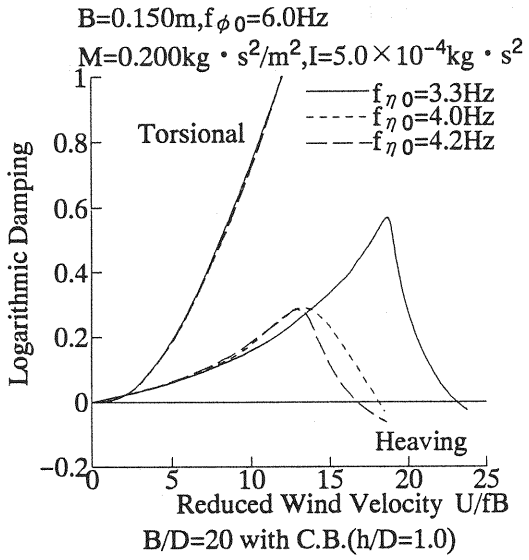

Fig.25 Effect of torsional/heaving natural ratio on branch

examined. The results are shown in **Fig.25**. Here it can be seen that flutter develops from the heaving branch in all cases. Therefore, it is believed that the branch from which flutter develops is inherent in each section.

9. CONCLUSION

The conclusions of this study are summarized as follows:

(1) Dependence between the aerodynamic derivatives

The following relationships of dependence that exist between the aerodynamic derivatives were examined.

(**a**) The dependence based on the similarity of unsteady pressure characteristics per unit angle of attack between heaving and torsional motion.

$H_3^*=H_1^*/k$, $H_2^*=-H_4^*/k$, $A_3^*=A_1^*/k$, $A_2^*=-A_4^*/k$

(**b**) The dependencies between H_1^* and H_4^*, H_2^* and H_3^*, A_1^* and A_4^*, A_2^* and A_3^*, based on the equivalent Wagner function.

When comparing the results of the eigen value analysis to which each dependence was applied with the original results of the analysis, it becomes clear that the two dependencies (a) and (b) are appropriate. Therefore, it is important for stabilization against flutter to control the characteristics of unsteady pressure around the body by giving consideration to these dependencies.

(2) Mechanism of coupled flutter

By examining the relationship between torsional motion and heaving motion through consideration of what roles the coupling terms posses, an attempt to clarify the mechanism of coupled flutter was made. In addition, the effect of the ratio between heaving and torsional natural frequency to the mode from which flutter develops was also examined. The conclusions are obtained as follows:

(**a**) In order to stabilize against flutter, it is necessary to keep the damping terms of 1DOF, A_2^*, and H_1^* negative. In addition, it is also considered that the coupling terms A_1^* and H_3^* play important roles in both cases where flutter develops from the heaving or torsional branch.

(**b**) The ratio between heaving and torsional natural frequency does not posses an influence upon the branch from which flutter develops. It is considered that the branch from which flutter develops is inherent in each section.

(3) The aerodynamic property of the elliptical section

Giving consideration to the fact that the slenderness ratio of the elliptical section is 3, this section possesses a capacity for resisting flutter. The most important factor of the favorable aerodynamic property is that the phase lag should be positive where the amplitude of fluctuating pressure $\tilde{C}_P$ becomes a maximum near the leading edge. Therefore, A_2^* becomes negative.

(4) The aerodynamic property of the rectangular section with a vertical plate

It became clear that the vertical plate improves stabilization against flutter. The most important factor of stabilization is the fact that the phase lag where $\tilde{C}_P$ becomes a maximum is improved.

(5) The aerodynamic property of the triangle section

It was found that the triangular section has almost the same flutter properties as the rectangular section with B/D=20, Giving consideration to the fact that the slenderness ratio of this section is 6, this section posses a high capacity for resisting flutter. The most important factor is the fact that the phase lag where $\tilde{C}_P$ becomes a maximum near the leading edge is negative, so that A_2^* becomes negative.

In the cases (3)~(5) shown above, the most important factor of the favorable aerodynamic property is the phase lag at the part where $\widetilde{C}_P$ is at its maximum.

(6) The aerodynamic property of the tandem ellipse

The aerodynamic properties of the tandem ellipse section became clear by using the forced vibration method. In addition, its stability against flutter was examined by use of the eigen value analysis.

(a) Under the hypothesis that the tandem ellipse takes the mode applied in this research, the flutter onset velocity could not be analyzed. However, under the mode applied in this research, the lift force of both sections caused by heaving velocity in torsional motion contributes to the aerodynamic damping in torsional motion and the lift force of both sections caused by torsional displacement cancel each other out. Therefore, it is expected that the tandem ellipse possesses a high capacity of flutter resistance.

(b) However it is difficult to realize the assumed mode in real bridges. It is necessary to examine the problem of the modes in order to apply the deck of the tandem ellipses to real bridges.

REFERENCES

1) Sato, H., Toriumi, R., Sekiya, M. and Watanabe, S. : Study on aerodynamic stability of super long-span bridge, *of 13th National Symposium on Wind Engineering*, pp.419-424, 1994.

2) Kusakabe, T., Sato, H. and Sekiya, M. : Ewperimental studies of the effect of the active control as flutter supressing device, *Proceedings of 13th National Symposium on Wind Engineering*, pp.431-436, 1994.

3) Matsumoto, M., Shiraishi, N., Shirato, H., Shigetaka, K., Niihara, Y. and Yamaguchi, S. : Aerodynamic derivatives of some structural sections, *Proceedings of 12th National Symposium on Wind Engineering*, pp.231-236,1992.

4) Scanlan,R.H.,Beliveau,J.G. and Budlong,K.S.:Indicial Aerodynamic Functions for Bridge Decks, Journal of the Engineering Mechanics Division, *Proceedings of ASCE.*,Vol.100,EM4,August, pp.657-672, 1974.

5) Matsumoto, M., Niihara, Y. and Kobayashi, Y. : On mechanism of flutter phenomena for structural sections, *Jounal of Structural Engineering*, Vol.40A, pp.1019-1024, 1994.

6) Matsumoto, M., Kobayashi, Y. and Hamasaki, H. : The role of flutterderivatives of flutter phenomena, *Proceedings of 13th National Symposium on Wind Engineering*, pp.377-382, 1994.

7) Matsumoto, M., Kobayashi, Y. and Hamasaki, H. : On mechanism of coupled flutter for fundamental bluffbodies, *Proceedings of 13th National Symposium on Wind Engineering*, pp.359-364, 1994.